

Adaptive dynamic sliding mode control for overhead crane for enhancing transient response

Qiang Hu ^{1, a}, Weimin Xu ^{2, *}

¹ Shanghai Maritime University, Shanghai 201306, China;

² Shanghai Maritime University, Shanghai 201306, China.

^a 1596417605@qq.com, ^{*} 1596417605@qq.com

Abstract

Most existing methods obtained with standard technique for overhead cranes with little consideration for enhancing the transient response when fulfilling the transportation tasks. Their performance may badly further degrade when it put into practical application. Therefore, this article proposes an adaptive dynamic sliding mode control for overhead crane for enhancing transient response solution for transportation objective of overhead cranes with varying rope length. The reference command signal, involves replacing the SMC discontinuous term with an adaptive PID term, which ensures that output signal has good transient indicators. Moreover, an adaptive moving sliding function, which achieves real-time adjustment of sliding manifold slope, is constructed to improve the rate of convergence. The asymptotic stability of the closed-loop system is backed up with rigorous Lyapunov-based analysis. Finally, the comparative simulation results further validate the feasibility and efficiency of the proposed scheme.

Keywords

Overhead cranes, adaptive sliding mode control, nonlinear sliding manifold, transient response.

1. Introduction

With fewer available actuators being equipped than the number of to-be-controlled degrees of freedom (DOFs), overhead cranes are typical known as underactuated systems with no direct control actions on the payloads, which have been widely founded and utilized as an important loading equipment for material transportation in various industrial fields, such as port transportation and equipment manufacturing [1-2]. Unfortunately, undesired payload swings occur for the inertia and various extraneous disturbances during the transportation of overhead crane system, which not only badly affects production efficiency, but also poses potential threats to surrounding machineries or cargos [3-4]. Currently, the solution to this problem relies on the practical operating experience of the skilled technicians. However, when cranes are manually manipulated, mistakes are usually inevitable and payloads often exhibit uncontrolled residual oscillations, which are very likely to trigger serious safety hazards. With the propose of solving the excessive dependence on operator experience, many researchers devoted their efforts to investigating the automatic control methods of overhead cranes, which has both great theoretical and practical significance.

After years of research, plenty of insightful high-performance control approaches have been made by a lot of researchers for the control of underactuated crane systems. The existing works on crane control can be roughly classified into two categories: trajectory planning (open-loop control) and feedback control design [3-5]. For the former, one of most extensively applied motion planning approaches is called the input shaping technique, which achieve transportation and anti-swing control objectives utilized linearized dynamics. In particular, in

[6], based on the particle swarm optimization algorithm, a methodology for designing controller in combination with an improved input shaping method is implemented to the control of three-dimensional overhead cranes, that achieves high oscillatory dynamics reduction during the transferring processes. Ref. [7] simultaneously imposes several constraints consisting of the allowable swing amplitude upon the payload, bounded velocity, acceleration, and even jerk upon the trolley, a novel offline minimum-time trajectory planning approach is proposed by means of the quasi-convex optimization technique. To achieve the objectives of safety and energy efficiency, Sun and Fang [8] disclosure an energy-optical solution for transportation control of cranes with double pendulum dynamics. Additionally, motion planning algorithms for overhead crane systems also have been reported based on the inherent nonlinear dynamical coupling behavior existing between the translational movement and the payload swing in literature [9-10]. Compared with the trajectory planning schemes, feedback control exhibits superior control performance with respect to parametric uncertainties and external disturbances. Many ambitious close-loop control strategies have been exploited for crane systems. Specifically, a series of control schemes are suggested on the basis of the passivity of the crane system in [11-13]. Assuming that velocity signals are unavailable, Lu et al. [14] propose an amplitude-saturated output feedback anti-swing algorithm for regulating double pendulum cranes, while Reference [15] proposes an interesting procedure generating swing-free nonlinear trajectories for crane systems. Also, taking into account the payload hoisting/lowering effect, in [16], a novel trajectory tracking control strategy is developed by carefully analyzing the system dynamics, which guarantees that anticipated performance metrics such as maximum swing angle, settling time, maximum trolley velocity/acceleration, and so forth. After that, Ref. [17] proposes a hybrid control scheme for the overhead cranes assuming that the system exists the viscous damping. Besides, feedback linearization, back-stepping, and optimal control have been utilized for anti-swing control assuming constant rope length [18-20]. Furthermore, abundant other efficient intelligent control algorithms including model predictive control [21], fuzzy logic control [22], learning control [23] and neural network based controllers [24] are also employed to enhance control performance, which also have promising prospects.

Though great efforts have been made on the anti-swing and positioning control of overhead cranes, there still exist many issues that require further investigation. For instance, overhead cranes, which exhibit under-actuated mechanism, complicated dynamic nonlinear behavior, along with complicated interactions among the motions, inevitably suffer from system parameter variations, and various extraneous disturbances from the working environment for practical applications, which usually induces severe performance (payload oscillation suppression effects and trolley positioning efficiency) degradation for many existing methodologies failing to consider these situations. To this end, sliding mode control (SMC) technique has been extensively employed in designing a robust controller for overhead crane systems due to its superior performance in inherent robustness, order reduction capability and disturbance rejection performance. Specifically, Ref. [25] suggests a robust nonlinear controller for overhead crane systems based on both conventional and hierarchical sliding mode techniques, both of which are discontinuous full state feedback controllers. More recently, an enhanced coupling PD with sliding mode control method is presented for double-pendulum overhead crane systems with considering unpredictable external disturbances in [26], that ensures asymptotic stability while keeping all state signals bounded. In addition, some sliding-mode based controller are also presented for controller design in regulation tasks.

Another main shortcoming when employing the SMC method for controller design, especially for an overhead crane, is that its dependence on the parametric uncertainty bounds (such as mass variations in the cart and the load). Nevertheless, it is transparent that model parameters on crane systems exhibit highly uncertain and nonlinear in practical scenarios, particularly

under the external disturbances. With the purpose of addressing this impracticality of utilizing the SMC control approach, some adaptive control strategies have been studied to calculate crane parameters online. Specifically, authors in [27] employ the Lyapunov stability theory to derive an adaptive technique against parametric uncertainties of an overhead crane. Besides, ref. [28] presents an adaptive tracking controller for double-pendulum overhead cranes despite parametric uncertainties and external disturbances, which guarantees that the trolley tracking error is within a prior set of boundary conditions and asymptotically converges to zero rapidly. Among various adaptive control structures, model reference adaptive control (MRAC) has received much attention. More precisely, Le et al. [29] exploit the model reference adaptive SMC (MRASMC) schemes for the 3D overhead crane and tower crane, respectively, to adaptively update the unknown and uncertain parameters, in which SMC guarantees system robustness while MRAC focuses on system adaptation. Nonetheless, the research on MRASMC for overhead cranes is still in its infancy and there exist many unresolved problems. Noting that these available MRAC control schemes only discuss the steady-state characteristics of control systems, while the tracking performance at the transient stage has been rarely analyzed, especially for overhead cranes control. However, the sluggish transient convergence response (such as overshoot, convergence rate) of the tracking error, particularly when the control system suffers from an abrupt change, will heavily degrade its safety and reliability. To the best of our knowledge, no successful cases on improving the transient response of the 2D overhead cranes have been reported so far.

Considering the background above, there exist many important issues that remain open and need further investigation for anti-sway and positioning control of overhead cranes. Therefore, in this article, the enhancement of overall system's transient response will be mainly pursued in the controller design to improve the dynamic characteristics of the closed-loop system. More contributions of the article are epitomized below:

- (1) To the best of our knowledge, the procedure for establishing controller based on SMC framework firstly focuses on reinforcing transient response. Compared to the previous research works on overhead cranes, adaptive control is explicitly investigated, extending the control attention from steady stage to transient phase.
- (2) The proposed MSM decides its slope dynamically, more successfully achieving faster convergence than the conventional sliding manifold.
- (3) The proposed method is robust to parameter uncertainties and control target changes

The rest of the paper is arranged as follows. Section 2 provides the system dynamics of the 2D overhead crane system and the problem formulation. The specific procedures of the controller design are available in Section 3. Section 4 illustrates some simulation results. Finally, some concluding remarks wrap up this work in Section 5.

2. System dynamics establishment and problem formulation

2.1. System dynamics establishment

The schematic diagram depicting the components of a 2D-overhead crane is shown in Figure 1. In the following, assuming the rope is massless, and the payload is considered as point mass.

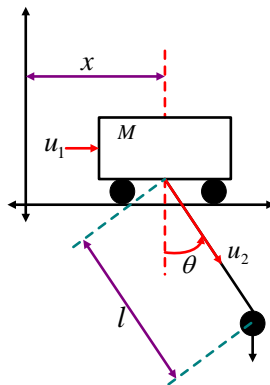


Figure 1: The schematic diagram of a two-dimensional overhead crane system

By utilizing the Euler-Lagrange formulation [36], the dynamics equation describing the physical behaviors of an underactuated overhead crane system are given by after elaborate calculations

$$(M + m)\ddot{x} - m \sin \theta \ddot{l} - ml \cos \theta \ddot{\theta} - 2m \cos \theta \dot{l} \dot{\theta} + ml \sin \theta \dot{\theta}^2 = u_1 \tag{1}$$

$$-m \sin \theta \ddot{x} + m \ddot{l} - ml \dot{\theta}^2 - mg \sin \theta = u_2 \tag{2}$$

$$-ml \cos \theta \ddot{x} + ml^2 \ddot{\theta} + 2ml \dot{\theta} + mgl \sin \theta = 0 \tag{3}$$

where $x(t) \in R^+$ represents the trolley displacement, $l(t) \in R^+$ is the variable rope length, and $\theta(t) \in R$ is the payload-swing angle. Signal $u_1(t) \in R$, $u_2(t) \in R$ correspond to the control input that allow the crane system to move along the horizontal plane, and varying the rope length, respectively. The elements $M \in R^+$, $m \in R^+$, g denote the trolley mass, the payload mass, and the gravitational constant, respectively.

Assumption 1: The payload swing angle is always within the following scope

$$-\pi/2 < \theta(t) < \pi/2 \tag{4}$$

The Equations (3) reflects the coupling relationship between the translational acceleration and the payload oscillations, i.e., they fully reveal how the trolley movement affects the swing motion.

Before proceeding with the subsequent analysis, some model transformations are performed. Equation (3) can be reorganized, after dividing both side with ml^2 , as follows

$$\ddot{\theta} = \frac{-g \sin \theta}{l} - \frac{2l \dot{\theta}}{l} + \frac{\ddot{x} \cos \theta}{l} \tag{5}$$

Then by inserting (5) into (1) and rearranging the resulting formula, which, along with Equation (2), after making some strict mathematical manipulations, further formulates the original actuated crane system (1) and (2) into the following nonlinear state-space form

$$\begin{cases} \dot{\varsigma}_1 = \varsigma_2 \\ \dot{\varsigma}_2 = \Pi(\varsigma_1, \varsigma_2) + \Lambda(\varsigma_1, \varsigma_2)u \end{cases} \tag{6}$$

with

$$\Pi(\varsigma_1, \varsigma_2) = \begin{bmatrix} 0 & g \cos \theta + l \dot{\theta} \end{bmatrix}^T, \Lambda(\varsigma_1, \varsigma_2) = \begin{bmatrix} \frac{1}{M} & \frac{\sin \theta}{M} \\ \frac{\sin \theta}{M} & \frac{M + m \sin^2 \theta}{Mm} \end{bmatrix} \tag{7}$$

wherein, $\varsigma_1 = [x, l]^T \in R^2$ corresponds to the system state variables, $u = [u_1 \ u_2]^T \in R^2$ denotes the control vector.

2.2. Problem formulation

This work aims to develop a control law such that the overhead crane system converges its desired position in the horizontal plane as well as hoisting/lowering a payload while restricting the magnitude of the swing angle. The control objective can be uniformly mathematically summarized as follows

Control objective: Design control law ensuring that limits

$$\lim_{t \rightarrow \infty} \{e(t), \theta\} = \{0, 0\} \tag{8}$$

hold, where $e(t) = \zeta_1 - \zeta_d$, $e_\theta(t) = \theta$, with $\zeta_d = [x_d, l_d]^T \in R^2$ being desired trolley position, the desired rope length reference signal, respectively.

3. Controller design

This section details the controller establishment with desirable transient performance and the corresponding stability analysis. To be specific, novel nonlinear sliding manifold is first introduced. Then, reference command signal developed based on adaptive sliding mode control (ASMC) generally makes the state variables converge to the desired equilibrium point, essentially indirect specifies a family of transient performance indicators for subsequent overhead cranes control. Additionally, we will discuss the asymptotic stability of reference model system. The schema (see Fig. 2) is described by the following block diagram.

To this end, consider the nonlinear sliding manifold (NLSM) $S = [s_x, s_l]^T \in R^2$, defined by

$$S = [\Gamma - \Phi P, I] \begin{bmatrix} e \\ \dot{e} \end{bmatrix} + H(\theta)\theta \tag{9}$$

where $x_d, l_d \in R^+$ denote the desired trolley position, the desired rope length signal, respectively.

$P = P^T \in R^{2 \times 2}$ corresponds to the positive definite matrix that can be determined by computing the following Lyapunov function

$$\Gamma^T P + P \Gamma = -\Xi \tag{10}$$

where $\Xi \in R^{2 \times 2}$ represents the positive definite matrix. $I^{2 \times 2}$ is an identity matrix. Let matrix Γ be a suitable full-rank matrix, which fulfills the Hurwitz theorem and provides small initial damping ratio for the reference model system. The nonlinear function $\Phi \in R^{2 \times 2}$ is diagonal matrix with non-positive nonlinear entries depending on reference model output and is utilized for regulating the damping ratio of the closed-loop system, which satisfies the following two properties:

(A1): It is supposed to be differentiable with respect to the output of reference model to ensure the existence of sliding mode.

(A2): Its value ought to change from zero to negative one.

Hence, we introduce the following nonlinear function Φ for controller development.

$$\Phi = \begin{bmatrix} -\xi_1 e^{-(x-x_d)^2} & 0 \\ 0 & -\xi_2 e^{-(l-l_d)^2} \end{bmatrix} \tag{11}$$

where $\xi_i, i = 1, 2$ are positive constants.

Likewise, one possible choice of vector H is

$$H(\theta_r) = [\nu + \xi_3 e^{-(\theta)^2} \quad 0]^T \tag{12}$$

with ν, ξ_3 being positive constants.

Remark 1: Unlike the conventional linear sliding manifold, the suggested nonlinear sliding manifold depends on the output so that the damping ratio of the system changes from its initial low value to its final high value as the output changes from its initial value to the set point. The initial low value of the damping ratio results in fast response, whereas the later high damping avoids overshoot to save energy consumption.

Then on the basis of the proposed nonlinear sliding manifold, we consider control input $u \in R^2$ as the next composed signal

$$u = u_L(t) + u_S(t) \tag{13}$$

where $u_L(t)$ is the equivalent law which is determined by $\dot{S} = 0$. The switching law $u_S(t)$ is selected such that

$$u_S(t) = -\Lambda^{-1}(\zeta)[u_{dis}] \tag{14}$$

where $u_{dis} = [q_x \text{sign}(s_x) \quad q_l \text{sign}(s_l)]^T$ with $q_i, i = x, l$ being positive constants.

Hence the control input given by (13) can be rewritten as follows

$$u = -\Lambda^{-1}(\zeta)[\Pi(\zeta) + [\Gamma - \Phi P]\dot{e} - \frac{d\Phi}{dt}Pe - \ddot{\zeta}_d + \frac{dH}{dt}\theta + H\dot{\theta} + u_{dis}] \tag{15}$$

where $\zeta_d = [x_d \quad l_d]^T \in R^2$

Remark 1: Despite the bigger q_i can guarantee sufficiently short time between reaching subsequent sliding manifold to achieve system rapid adjustment by shortening the reaching phase, it inevitably induces the serious chattering. Conversely, when small values are chosen for q_i , this yields a slower convergence speed. Thus, there exists an inherent tradeoff between the convergence speed of tracking error and the chattering, which cannot be easily managed by employing control input. Motivated by this fact, in what follows, the discontinuous term is replaced by an adaptive PID term to improve the transient response and attenuate the chattering phenomenon.

$$u_{sw} = -\Lambda^{-1}(\zeta)u_{PID} \tag{16}$$

Then the adaptive term can be described as the next architecture:

$$\begin{aligned} u_{PID} = \rho(S, \mathcal{G}) &= \begin{bmatrix} k_{px}s_x + k_{ix} \int_0^t s_x(\nu)d\nu + k_{dx} \frac{d}{dt}s_x \\ k_{pl}s_l + k_{il} \int_0^t s_l(\nu)d\nu + k_{dl} \frac{d}{dt}s_l \end{bmatrix} \\ &= [\rho_x(s_x, \mathcal{G}_x), \rho_l(s_l, \mathcal{G}_l)]^T \\ &= [\mathcal{G}_x^T \Psi(s_x), \mathcal{G}_l^T \Psi(s_l)]^T \\ &= \Psi(s) \mathcal{G} \end{aligned} \tag{17}$$

where $\mathcal{G}_i = [k_{pi} \quad k_{ii} \quad k_{di}]^T$, $\mathcal{G} = [\mathcal{G}_x^T \quad \mathcal{G}_l^T]^T$, $\Psi(s_{2i}) = [s_i \quad \int_0^t s_i(\nu)d\nu \quad \frac{d}{dt}s_i]^T$ and $\Psi(S_2) = \text{diag}[\Psi^T(s_x) \quad \Psi^T(s_l)]$ with k_{pi}, k_{ii} and k_{di} are the tunable gains.

We can ultimately formulate the reference input u_r into the following manner

$$u = -\Lambda^{-1}(\zeta)[\Pi_0(\zeta) + [\Gamma - \Phi P]\dot{e} - \frac{d\Phi}{dt}Pe - \ddot{\zeta}_d + \frac{dH}{dt}\theta + H\dot{\theta} + \rho(S, \mathcal{G})] \tag{18}$$

The parameter vectors are computed employing the following adaptation laws

$$\dot{\mathcal{G}} = \chi_g \Psi(S)S \tag{19}$$

where $\chi_g > 0$ denotes the adaption gain.

Based on the previous development, we establish the following theorem which states that the control objective (8) is achieved by utilizing controller (18).

Theorem : Let the overhead crane model (5), (6) driven by controller (18). Then, state variable x_d, l_d asymptotically converge to their desired values x_d, l_d respectively, and simultaneously attenuate the payload swing angle, which can be mathematically expressed as

$$\lim_{t \rightarrow \infty} [e \ \theta] = [0 \ 0] \tag{20}$$

Proof: Define the optimal parameters vector:

$$\mathcal{G}_i^* = \arg \min_{\mathcal{G}_i \in \Omega_i} (\sup_{s_i \in R} \| q_i \text{sign}(s_{2i}) - \rho_i(s_i, \mathcal{G}_i) \|); i = x, l \tag{21}$$

where Ω_i are the constraints set for \mathcal{G}_i .

Assuming that the constraints set Ω_i above are specified as follows

$$\Omega_i = \{ \mathcal{G}_i : \| \mathcal{G}_i \| < M_{\mathcal{G}_i} \} \tag{22}$$

where $M_{\mathcal{G}_i}$ corresponds to the predefined parameter.

w_i represents the minimum approximation errors defined as

$$w_i = q_i \text{sign}(s_{2i}) - \rho_i(s_{2i}, \mathcal{G}_i^*) \tag{23}$$

Denote:

$$W_{PID} = [w_x \ w_l]^T \tag{24}$$

The approximation error vector belongs to $L_2[0, t], \forall t > 0$, with $\| W_{PID} \| \leq W_{PIDmax}$

Differentiating nonlinear sliding manifold S_2 with respect to time, it yields

$$\begin{aligned} \dot{S} &= -\rho(S, \mathcal{G}) + W_{PID} - q \text{sign}(S) + \Psi(S)\mathcal{G}^* \\ &= \Psi(S)\mathcal{G} + W_{PID} - q \text{sign}(S) \end{aligned} \tag{25}$$

Where $\mathcal{G} = \mathcal{G}^* - \mathcal{G}$.

Let us consider the nonnegative Lyapunov function candidate

$$V = \frac{1}{2} \text{tr}(S^T S) + \frac{1}{2\gamma_g} \text{tr}(\mathcal{G}^T \mathcal{G}) \tag{26}$$

Taking the time derivatization of V results in

$$\dot{V} = \text{tr}(S^T \dot{S}) + \frac{1}{\gamma_g} \text{tr}(\mathcal{G}^T \dot{\mathcal{G}}) \tag{27}$$

by inserting (25) into (28) and integrating the terms by parts, we have

$$\begin{aligned} \dot{V} &= \text{tr} \left(S^T \left(\Psi(S)\mathcal{G} + W_{PID} - q \text{sign}(S) \right) \right) + \frac{1}{\gamma_g} \text{tr}(\mathcal{G}^T \dot{\mathcal{G}}) \\ &= \text{tr}(S^T \Psi(S)\mathcal{G}) - \text{tr}(S^T q \text{sign}(S)) + \text{tr}(S^T W_{PID}) + \frac{1}{\gamma_g} \text{tr}(\mathcal{G}^T \dot{\mathcal{G}}) \end{aligned} \tag{28}$$

From the fact that

$$\text{tr}[S^T \Psi(S)\mathcal{G}] = \text{tr}[\mathcal{G}^T \Psi(S)^T S] \tag{29}$$

We have $\dot{\mathcal{G}} = -\dot{\mathcal{G}}$, noting $q_s = \sum_{i=x,l} q_i$

Hence, we can rewrite (27) as

$$\dot{V} = tr(\mathcal{G}^T (\Psi^T(S)S - \frac{1}{\gamma_g} \dot{\mathcal{G}}) - q_s tr(S^T sign(S)) + tr(S^T W_{PID})) \tag{30}$$

Applying the results in (28) to (29) produces

$$\begin{aligned} \dot{V}_1 &= -q_s tr(S^T sign(S)) + tr(S^T W_{PID}) \\ &\leq -q_s |S| + |S| W_{PIDmax} \end{aligned} \tag{31}$$

with $sign(S) = [sign(s_x) \quad sign(s_l)]^T$, and $|S| = \sum_{i=x,l} s_i$

To render V negative definite, i.e., $\dot{V} \leq 0 \Rightarrow V(t) \leq V(0)$, we can conclude that $q_s \geq W_{PIDmax}$, implying that $S, \mathcal{G} \in L_\infty$. From (24), one further derives that $\dot{S} \in L_\infty$.

By integrating both sides of (30) we can upper bound $V(t)$ as follows

$$V(t) \leq V(0) - q_s \int_0^t |S(\nu)| d\nu \tag{32}$$

Since $V(t), V(0) \in L_\infty$, relation (31) entails that $\lim_{t \rightarrow \infty} \int_0^t |S(\nu)| d\nu \in L_\infty$, together with $\dot{S} \in L_\infty$, based on Barbalat's lemma, one can infer that $\lim_{t \rightarrow \infty} S \rightarrow 0$, which further indicates that

$$\lim_{t \rightarrow \infty} [e \quad \theta] = [0 \quad 0] \tag{33}$$

which completes the proof, and demonstrates that the control objective (8) is achieved.

4. Simulation results and analysis

This Section presents the numerical simulation results validating the effectiveness of the proposed approach. More precisely, super-twisting sliding mode controller (STSMC) [23] and the adaptive sliding mode controller [31] are taken as the comparison. Then, the robustness with respect to different/uncertain payload masses, rope lengths is verified via MATLAB/Simulink 2017b environment.

For all the simulations, unless otherwise stated, the related inertial parameters are set as follows

$$M = 2kg, m = 0.8kg, g = 9.81kg / s^2$$

and the initial/final conditions are selected as follows

$$x_0 = 0m, l_0 = 0.1m, x_d = 1m, l_d = 0.8m$$

4.1. Comparison with existing methods

The results of the first group of simulation results are shown in Fig.2.

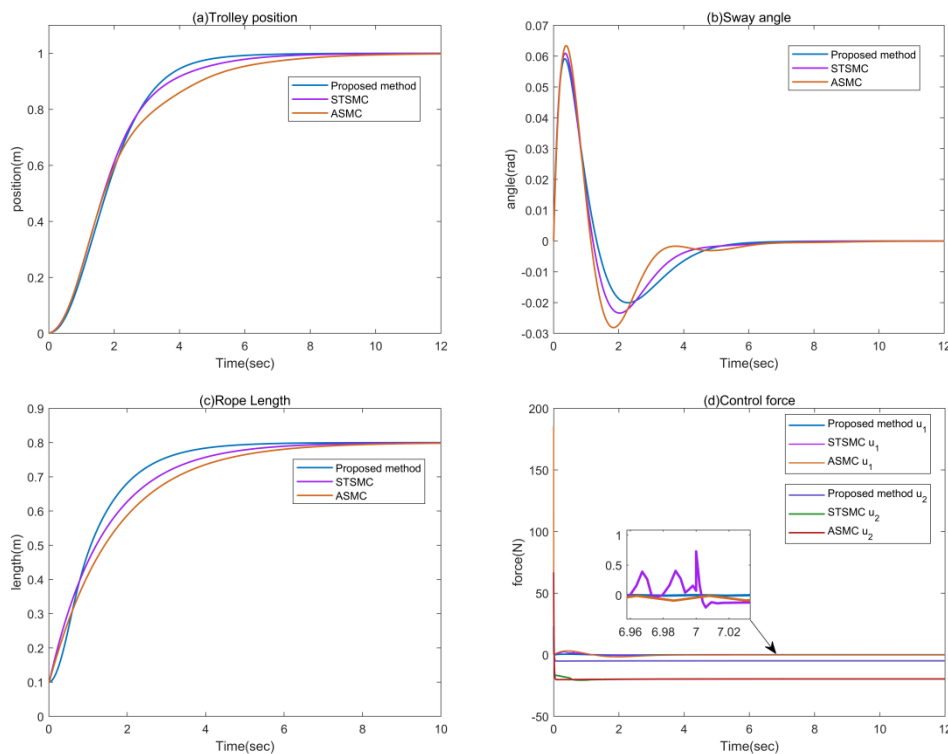


Figure 2: Simulation results of the different methods.

As seen from Fig(a)and(b), the trolley accurately and rapidly reaches the desired location within about 6.7 s, and there are no residual payload oscillations. Therefore, the proposed controller achieves the control objective and satisfactorily guarantees the physical behaviors, such as maximum velocity/acceleration, as well as swing amplitudes. In contrast, the trolley by comparison methodologies reaches the same desired location within about 8-10 s, which is slower than the proposed method. Moreover, the payload sways more severely, which may result in safety risks. In addition, from Fig.2(d), the control input u_1 of STSMC and ASMC exhibits more or less chattering phenomenon, while the control input of proposed method does not suffer from chattering

In general, compared with the results of the STSMC and ASMC controllers shown in Figs. 2(a), (b) and (c), the proposed method attains better performance in the following aspects:(1) It can suppress the residual swing effectively over the comparative methods, as shown in Fig. 2(b) and

4.2. Robustness verification against parameter uncertainties

In this subsection, the robustness against parameter uncertainties of the proposed method is verified, while the other parameter values are kept the same as before, except that system parameters and initial/final conditions. To this end, the following two cases of simulation experiments are carried out:

Case 1: Parameter uncertainties. The system parameters are changed to $M = 5kg$, $m = 2kg$,respectively, while their nominal values are still $M = 2kg$, $m = 0.8kg$

Case 2: Two different transportation task. The initial and target positions for the overhead cranes are changed to $x_0 = 0.01m$, $l_0 = 0.2m$, $x_d = 1.2m$, $l_d = 1m$ (and $x_d = 1.5m$, $l_d = 1.2m$)

Limited by the paper length, the figures for the control inputs are not provided in Figs., since they are very similar with those in the first set of simulations.

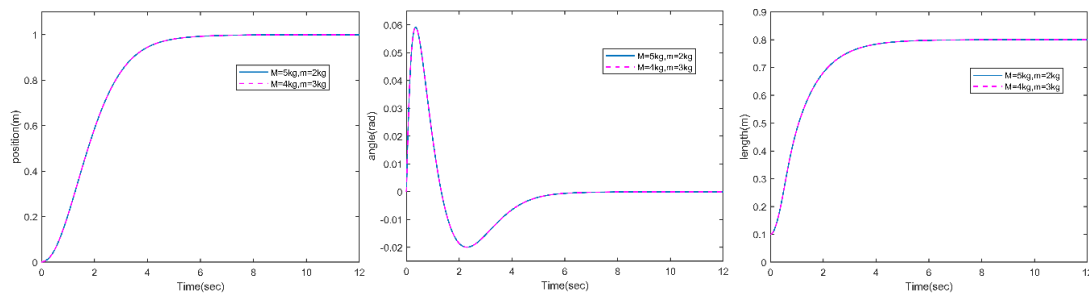


Figure 2: Simulation results: test of parameter uncertainty

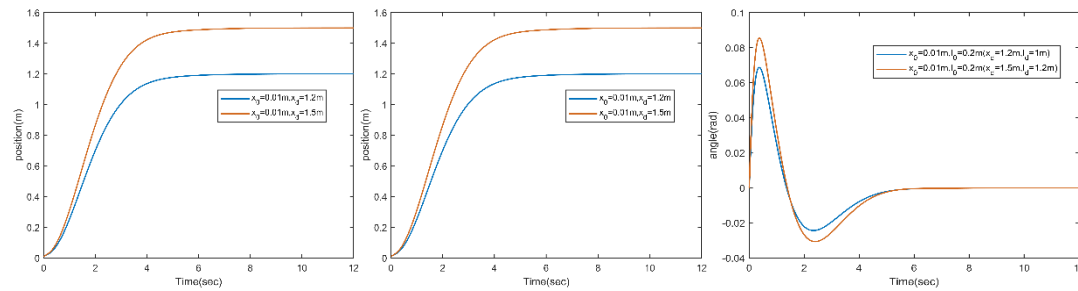


Figure 3: Simulation results: test of a different transportation task

The simulation results for Cases 1.2 are collected in Fig.3. It can be observed from Fig.(a), (b)and(c) that, even in the presence of various parameter uncertainties, the proposed approach still achieves satisfactory control performance, namely, the trolley accurately reaches the desired location with no residual angle swings. Furthermore, from the results in Fig4. (a), (b)and(c), one can conclude that the simulation experiment carried out intentionally in Case2 further validates the proposed approach’s adaptability to different transportation tasks. To sum up, as indicated by simulation experimental results, the proposed method has satisfactory robustness toward system parameter uncertainties or even different control objectives.

5. Conclusion

In this paper, an adaptive dynamic sliding mode control scheme is proposed for anti-sway and positioning control of a two-dimensional overhead crane with variable rope length. In terms of controller design, the designed nonlinear sliding mode surface can which achieves real-time adjustment of sliding manifold slope, is constructed to improve the rate of convergence. Then the proposed control strategy can suppress the parameter varying occurring in the overhead crane. Moreover, the designed MSMS improves the convergence rate of state variable errors. The stability of controller is strictly proven by Lyapunov stability theory. Finally, two kinds of simulation experiments are carried out for showing the efficiency of the proposed controller, and the simulation studies demonstrate that the controller in can make the system state variable errors converge to zero rapidly, besides, this control scheme also suffers from fewer chattering phenomenon as compared to other previous control strategy. In the future work, we will commit to expanding the application of the proposed approach for the control of a series of underactuated systems.

References

- [1] J. Kim, D. Lee, B. Kiss and D. Kim: An adaptive unscented Kalman filter with selective scaling (AUKF-SS) for overhead cranes. IEEE Transactions on Industrial Electronics, Vol. 68(2021), No.9, p. 6131-6140.

- [2] H.Ouyang, B.Zhao and G.Zhang: Enhanced-coupling nonlinear controller design for load swing suppression in three-dimensional overhead cranes with double-pendulum effect. *ISA Transactions* Vol.115(2021), No.5, p. 95-107.
- [3] V. D. La and K. T. Nguyen: Combination of input shaping and radial spring-damper to reduce tridirectional vibration of crane payload. *Mechanical Systems Signal Processing*. Vol.116 (2019), No.8, No.789, p. 310–321.
- [4] H. I. Jaafar, Z. Mohamed and M. A. Shamsudin: Model reference command shaping for vibration control of multimode flexible systems with application to a double-pendulum overhead crane, *Mechanical Systems Signal Processing*. Vol.115 (2019), No.89, p. 677–695.
- [5] S. M. Fasih, Z. Mohamed and A. R. Husain: Payload swing control of a tower crane using a neural network-based input shaper, *Measurement & Control*. Vol.25 (2019), No.56, p. 624–635.
- [6] E. Khorshid, A. A. Fadhli: Optimal command shaping design for a liquid slosh suppression in overhead crane systems, *Journal of Dynamic Systems Measurement and Control Transactions of the ASME*. Vol.68 (2018), No.45, p. 38–57.
- [7] X. Zhang, Y. Fang, N. Sun: Minimum-time trajectory planning for underactuated overhead crane systems with state and control constraints, *IEEE Transactions on Industrial Electronics*. Vol.55 (2017), No.6, p. 22–37.
- [8] N. Su, Y. Wu and C. He: An energy-optimal solution for transportation control of cranes with double pendulum dynamics: Design and experiments, *Mechanical Systems & Signal Processing*. vol.54 (2018), No.56, p. 64–55.
- [9] H. D. Tho, A. Kaneshige and K. Terashima A: Minimum-time S-curve commands for vibration-free transportation of an overhead crane with actuator limits, *Control Engineering Practice*. Vol.41 (2018), No.56, p. 333–354.
- [10] x.Wang, J. Liu and X. Dong: An energy-time optimal autonomous motion control framework for overhead cranes in the presence of obstacles, *Proceedings of The Institution of Mechanical Engineers Part C-Journal of Mechanical Engineering Science*. Vol.134 (2020), No.77, p. 333–354.
- [11] F. Villaverde, C. Raimundez and A. Barreiro: Passive Internet-based Crane Teleoperation with Haptic Aids, international journal of control and automation system, *International Journal of Control Automation and Systems*. Vol.5 (2020), No.54, p. 23–33.
- [12] H. Chen, B. Xuan, and P. Yang: A new overhead crane emergency braking method with theoretical analysis and experimental verification, *Nonlinear Dynamics*. vol.7 (2021), No.78, p. 367–378.
- [13] P. Shen, J. Schatz and R. Caverly: Passivity-based adaptive trajectory control of an underactuated 3-DOF overhead crane, *Control Engineering Practice*. Vol.121 (2018), p. 68–79.
- [14] N. Sun, Y. Fang, H. Chen and B. Lu: Amplitude-saturated nonlinear output feedback anti-swing control for underactuated cranes with double-pendulum cargo dynamics, *IEEE Transactions on Industrial Electronics*. Vol.34 (2018), p. 68–79.
- [15] T. Yang, H. Chen and Y. Fang: Motion trajectory-based transportation control for 3-D boom cranes: analysis, design, and experiments. *IEEE Transactions on Industrial Electronics*, Vol.12(2019), No.6, p. 90-102.
- [16] R. Miranda-Colorado and L.T. Aguilar: A family of anti-swing motion controllers for 2D-cranes with load hoisting/lowering. *Mechanical Systems & Signal Processing*, Vol.2(2018), No.6, p. 91-100.
- [17] L. Ramli, Z. Mohamed, M.Ö. Efe, I.M. Lazim and H.I. Jaafar: Efficient swing control of an overhead crane with simultaneous payload hoisting and external disturbances. *Mechanical Systems & Signal Processing*, Vol.79(2018), No.8, p. 19-22.
- [18] L. A. Tuan, S. G. Lee and V. H. Dang: Partial feedback linearization control of a three-dimensional overhead crane. *International Journal of Control Automation and Systems*, Vol.9(2017), No.98, p. 9-19.
- [19] K. Oh, J. Seo and J. G. Kim: MPC-based Approach to Optimized steering for minimum turning radius and efficient steering of multi-axle crane. *International Journal of Control Automation and Systems*, Vol.15(2017), No.4, p.29-33.

- [20] D. Sturzer, A. Arnold and A. Kugi: Closed-loop stability analysis of a gantry crane with heavy chain and payload. *International Journal of Control*, Vol.34(2019), No.6, p.21-35.
- [21] G. Galuppini, L. Magni and D. M. Raimondo: Model predictive control of systems with dead zone and saturation. *Control Engineering Practice*, Vol.54(2020), No.7, p.36-45.
- [22] Q. H. Ngo, N. P. Nguyen and Q. B. Truong: Application of fuzzy moving sliding surface approach for container cranes. *International Journal of Control Automation and Systems*, Vol.34(2019), No.6, p.21-35.
- [23] T. Yang, H. Chen and Y. Fang: Motion trajectory-based transportation control for 3-D boom cranes: analysis, design, and experiments. *IEEE Transactions on Industrial Electronics*, Vol.12(2019), No.6, p. 90-102.
- [24] X. Zhang, Y. Fang, N. Sun: Minimum-time trajectory planning for underactuated overhead crane systems with state and control constraints, *IEEE Transactions on Industrial Electronics*. Vol.55 (2017), p. 22–37.
- [25] V. D. La and K. T. Nguyen: Combination of input shaping and radial spring-damper to reduce tridirectional vibration of crane payload. *Mechanical Systems Signal Processing*. Vol.116 (2019), No.8, p. 310–321.
- [26] L. Rincon, Y. Kubota and G. Venture: Inverse dynamic control via "simulation of feedback control" by artificial neural networks for a crane system. *Control Engineering Practice*, Vol.65 (2019), p. 24–35.
- [27] L.A. Tuan and S.G. Lee. Sliding mode controls of double-pendulum crane systems, *Journal of Mechanical Science and Technology*. Vol.106 (2019), No.9, p. 300–321.
- [28] Zhang: An Enhanced coupling PD with sliding mode control method for underactuated double-pendulum overhead crane systems. *International Journal of Control and Automation System*, Vol.55 (2020), p. 66–78.
- [29] A. M. Singh, Q. P. Ha: Fast terminal sliding control application for second-order underactuated systems, *International Journal of Control and Automation System*, Vol.65 (2021), p. 7–18.